Jurnal Teknologi, 32(F): 77–92
© Universiti Teknologi Malaysia

THE EFFECT OF HYDROGEN REDUCTION TEMPERATURES ON THE PALLADIUM-SUPPORTED CATALYST IN THE COMBUSTION OF METHANE

NOOR SHAWAL NASRI[1], RAHMAT MOHSIN[2] & AZEMAN MUSTAFFA[3]

Abstract. The effect of hydrogen reduction temperatures was investigated using alumina-supported palladium for its catalytic activity in the catalytic combustion of methane. The change of total BET surface area showed that reduction temperature at 673K gave the highest surface area, then followed by 533K, and lastly by 773K. The surface area changed by 673K showed the optimum activity as compared to the others. Hydrogen reduction at different temperatures caused the different of oxidation and reduction states of palladium qualitatively, as shown in XPS results. The metallic and ionic species present in reduced samples have influence in the catalyst performance during methane oxidation. In conjunction with TEM study indicated that 773K contributed a serious sintering problem. The optimum particle size was obtained at 673K for optimum methane conversion under chemical kinetic regime, then followed by 533K, and lastly at 773K.

Abstrak. Kesan suhu penurunan hidrogen telah diselidiki menggunakan paladium berpenyokong-alumina untuk kesan keaktifan mangkin dalam pembakaran bermangkin metana. Perubahan jumlah luas permukaan BET menunjukkan suhu penurunan pada 673K telah memberikan luas permukaan tertinggi, kemudian diikuti 533K, and akhir sekali 773K. Perubahan luas permukaan pada 673K menunjukan aktiviti optima dibandingkan dengan lain. Penurunan hidrogen pada suhu berbeza menyebabkan perubahan pada keadaan pengoksidanan dan penurunan paladium secara kualititi, seperti yang ditunjukkan oleh keputusan XPS. Pembentukan spesis metalik dan ionik dalam sampel terturun mempengaruhi kecekapan mangkin semasa pengoksidanan metana. Bersama dengan kajian TEM, menunjukkan suhu 773K menyumbangkan masalah pembesaran partikel yang parah. Saiz partikel optima telah diperolehi pada 673K bagi penukaran metana optima untuk regim kinetik kimia, kemudian diikuti 533K, dan akhir sekali 773K.

Key Words: Supported-palladium, reduction-temperatures, catalyst, sintering, BET surface area, methane-oxidation

1.0 INTRODUCTION

Precious metal group catalysts are used in a number of applications such as in three way catalytic converters in exhaust vehicles, and in combustion process. Palladium supported catalyst shows high performance in methane conversion

[1,2,3] Gas Engineering Department, Faculty of Chemical Engineering and Natural Resources Engineering, Universiti Teknologi Malaysia, 81310 UTM Skudai, Johor Darul Ta'zim.

compared to other precious metal group catalysts such as rhodium and platinum [1]. The nature of palladium supported catalyst plays an important role in the performance of the catalyst activity such as it may change due to reaction structure sensitivity [2], oxidation state [3,4], and morphological effects [5,6]. Furthermore, the catalytic activity of palladium supported may deactivate during the combustion process. The main modes of the catalyst deactivation can be known as sintering [7], spinal formation [8], PdO or Pd sintering [9], or transformation of PdO to Pd [10]. The catalyst deactivation such as due to metal sintering could reduce high catalytic activity. Catalyst atmosphere such as in hydrogen environment will cause this sintering problem [11]. This sintering phenomenon is also influenced by temperature and time, hence could alter the catalyst structure and activity. One reason that the effect of catalyst activity may also change is because of different material supports used which cause the different effect behaviour. The effect of different behaviour catalyst supports for oxidation of methane on palladium supported on alumina, silica gel and molecular sieve have been reported [5,12].

This study was carried out to investigate the effect of hydrogen atmosphere at different temperatures on the supported-palladium catalyst in the combustion of methane, especially the sintering phenomenon affects on the catalytic activity. The total surface area, metallic and ionic species present, and microstructure were identified by BET, XPS and TEM, respectively. A plug flow micro-reactor was used to measure the level of methane conversion from 0 to 100%. The mass-specific rate was calculated under chemically kinetic regime at 623K for the purpose of comparison among the reduction temperatures.

2.0 MATERIAL AND METHOD

2.1 Catalyst Preparation

2 wt% Pd was supported onto the dry support of γ-alumina by using a wet impregnation method of $Pd(NO_3)_3.H_2O$ solution. Eventhough this is one of the simplest and most direct deposition methods, catalysts pores can be filled with metal salt solution [13]. Catalyst was prepared in an individual batch of 10 g. After mulling the γ-alumina support with the metal salt solution, the solid was allowed to air dry at room temperature. The catalyst was then calcined under a constant airflow using a Eurotherm tube furnace equipped with a programme controller. At the beginning of the calcination process, the sample was heated at a rate of 4°C/min until 475°C and held at this temperature for 240 minutes. It was then cooled at 10°C /min to 25°C. The calcined of 2 wt% metal/γ-alumina catalyst was then sieved to produce the particle size of < 100 mesh.

2.2 Catalyst Characterization

Four different samples were studied in order to characterize them, i.e. one calcined Pd/Al_2O_3 (CaPd) and three different reduced Pd/Al_2O_3 samples. The different reduced samples had been reduced for three hs with 3.6 L/min H_2 at different reduction temperatures, i.e. 533K (Pd533), 673K (Pd673) and 773K (Pd773) prior to characterize.

Three methods were carried out in order to characterize the calcined and hydrogen reduced samples. The total surface area was measured by using BET theory, whereas the oxidation state present was identified by using XPS technique and the instrument used was electron spectroscopy chamber VG Escalab. The metal sintering effect was carried out by using transmission electron microscopy (TEM) technique, model: Phillips CM20.

Table 1 shows the total BET surface area obtained for the calcined and reduced samples. The results for the surface analysis of the metallic and ionic species present in calcined and H_2-reduced Pd/Al_2O_3 samples are shown in Table 2 and 3 respectively. Figure 2 shows the TEM results for the micro-structure study.

Table 1 Total BET Surface Area of Calcined and Reduced Samples, and % Changed of Reduced Samples with Respect to Calcined Sample

Samples	BET Surface Area/m^2g^{-1}	% Change of BET Surface Area
CaPd	108	–
Pd533	134	+ 24
Pd673	152	+ 41
Pd773	130	+ 22

Table 2 Ratio of Reduced-calcined of Metallic Phase Present

Samples	Metallic Phase		Reduced/Calcined Ratio
	Binding Energy/eV	Area/counts	
CaPd	334.8	20152	1.00
Pd533	335.3	12823	0.64
Pd673	335.2	10995	0.55
Pd773	335.3	10717	0.53

Table 3 Ratio of Reduced-calcined of Ionic Phase Present

Samples	Ionic Phase		Reduced/Calcined Ratio
	Binding Energy/eV	Area/counts	
CaPd	340.1	10403	1.00
Pd533	340.6	9242	0.89
Pd673	340.5	7497	0.72
Pd773	340.7	7771	0.75

2.3 Catalytic Oxidation of Methane

Two conditions have been applied in order to study the catalyst activity by using a plug flow micro-reactor. The conditions are: (i) calcined (CaPd) and (ii) freshly reduced with hydrogen at 533K (Pd533), 673K (Pd673), and 773K (Pd773).

The catalyst performance was examined by setting up the test rig combustion facility as shown in Figure 1. The reduction process was done in-situ prior to methane combustion. The total flow rate of feed was 100 mL/min with 4.25 ± 0.25 vol. % of methane (CH_4) gas, the balance was oxygen (O_2) and nitrogen (N_2) gases. The feed gases CH_4, O_2, and N_2 and gas combustion products such as carbon monoxide (CO), carbon dioxide (CO_2), O_2, N_2, H_2 were analysed by off-line gas chromatography.

Figure 3 shows the isothermal methane conversion from 0 to 100% conversion as a function of catalyst temperature whereas Figure 4 shows the Arrhenius plots for methane conversion less than 50%.

3.0 RESULTS AND DISCUSSION

3.1 Total BET Surface Area

Hydrogen reduction at different temperature for 3 hs has affected and changed the morphology of all the catalysts studied. Table 1 shows the BET surface area of all reduced catalysts. Pd/Al_2O_3 samples reduced at 533K, 673K, and 773K showed increases of BET surface area of 24%, 41%, and 22%, respectively, compared to calcined Pd/Al_2O_3.

The increase of surface area may be due to the movement of particles in the alumina-support i.e. from the pores during the hydrogen reduction process to surface, and a decrease of metal particle size, i.e. an increase in particle dispersion. However, the increase in reduction temperature may cause the collision of particles, which then coalesce. Larger particles would result in the

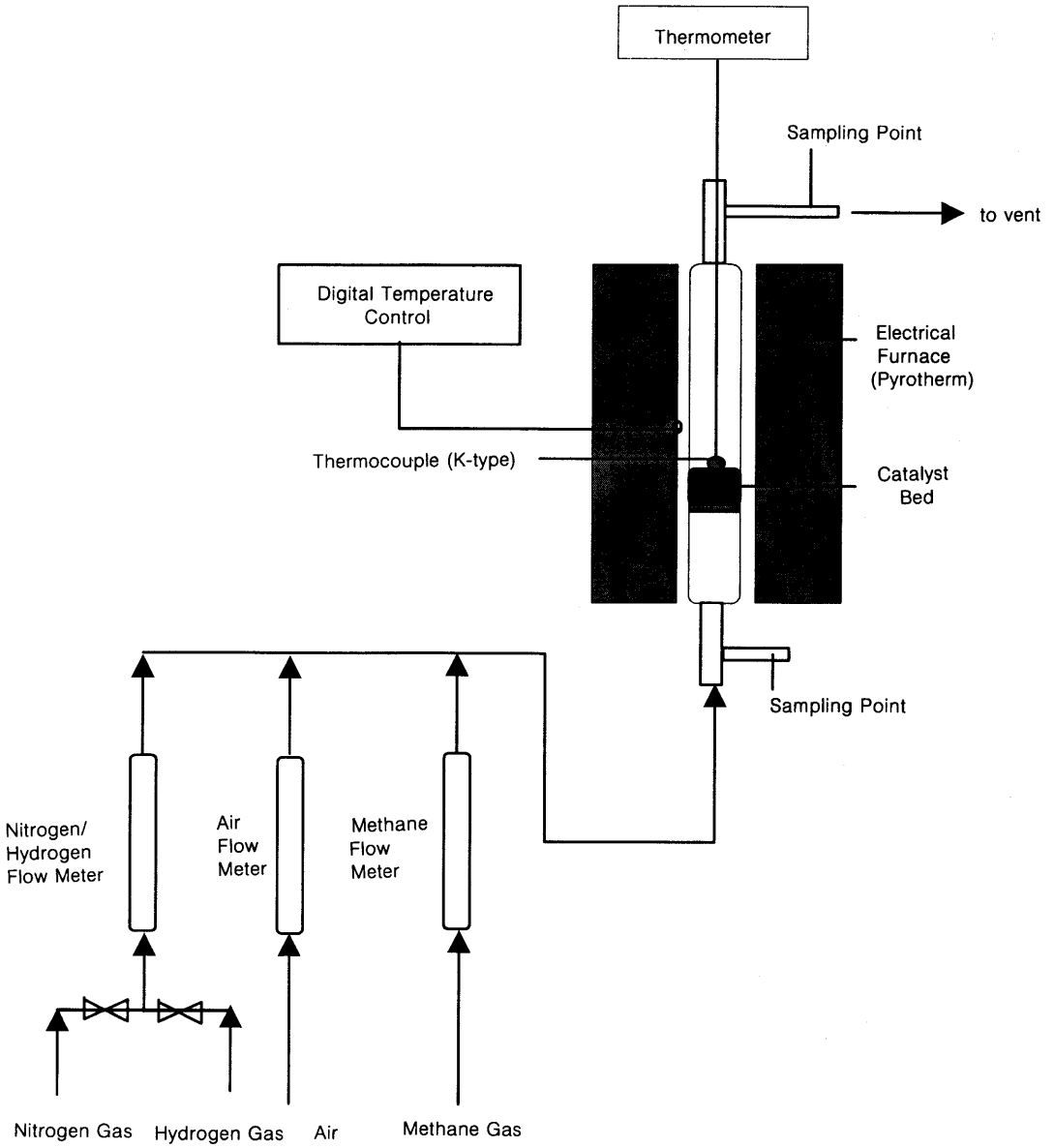

Figure 1 Schematic Layout of the Rig of the Methane Catalytic Combustion

increased of pore blockage and thus lower surface area. Such a mechanism for particle growth would be reflected in the surface area of the sample as seen for the catalyst reduced at 773K. The details of the particle growth mechanism have been determined by the TEM study discussed in the next section. The increase in surface area suggest an optimum in the particle size of metallic and/

or ionic phases present on the support surface. Hence, it may be expected that this change in the catalyst nature also affects its activity, i.e. an increase in catalyst activity, as identified in catalyst activity section.

3.2 Oxidation State by X-Ray Photoelectron Spectroscopy

The XPS study concerned the binding energy of the metallic and ionic phases for the calcined, and reduced catalysts. The presence of other species such as oxygen, aluminium, sulphur and carbon are not considered here. Metallic and ionic species present in the treated precious metal catalysts have to be considered in terms of the relative ratios. The XPS peaks obtained and assigned for metallic and ionic species are not shown in this report. Tables 2 and 3 show the ratio of reduced to calcined samples of metallic and ionic present, respectively, at different reduction temperatures.

It can be noted that during the reduction process, ionic and metallic species have been changed and dispersed, thus the nature of the catalysts has been modified, and ionic reduction has possibly occurred. The standard range of binding energies for precious metal catalysts has been reported [14]. The binding energy of the metallic phase (Pd) of Pd/Al_2O_3 is in the range of 334.8-335.3 eV, and the binding energies for the ionic phase of Pd shift to 340.1-340.7 eV. The metallic-ionic ratios may have an influence on the catalytic combustion of methane, as discussed in detail in section of catalyst activity.

The Pd/Al_2O_3 sample (calcined) without any reduction showed the highest metallic fraction compared to the ionic phase. This is surprising since reduction is expected to increase the M^o/M^{n+} ratio. The decrease in the metallic species in Pd533, Pd673 and Pd773 may be due to the re-oxidisation to ionic species prior to the XPS study in which the reduced samples have been exposed to atmospheric condition.

3.3 Metal Sintering by TEM Study

The effect of sintering from the hydrogen reduction at different temperatures is an important aspect because the sintering phenomenon degrades the catalyst life. Sintering behaviour takes place when metallic or crystallite, or ionic phases move on the substrate surface, and where metallic or ionic molecules may form transitory and mobile molecular intermediates. Ionic oxides may also diffuse along the support surface or through the vapour phase, from higher energy sites to lower energy sites. Hydrogen, inert, or oxygen atmospheres have different sintering patterns. It has been noted that the sintering rate is larger in an oxygen atmosphere than in a hydrogen atmosphere [15, 16]. The presence of water either in gas phase or from the support, during the reduction of calcined supported catalysts also induces sintering [17].

Figure 2 shows the micro-structure of 2 wt% Pd/Al_2O_3 reduced at 533K,

673K and 773K after 3 hours under 3.6 L/h hydrogen. This TEM study shows the morphology of the catalyst under different reduction temperatures. It is clear that the surface structure has changed in terms of both particle sizes and topology.

Figure 2 (A) shows that reduction at 533K generates a catalyst in which the metal particles are uniformly distributed as individual particles on the substrate with a monomer particle dispersion. It shows some isolated particles for which the average particle size can be estimated as 10-13 nm. Some particles are suggested arise from migration, presumably via transitory of mobile particle intermediates. Reduction at 533K showed that monomer dispersion happened as individual particles are equally distributed on the surface of the support. These individual onomer particles may detach to form twinning particles, move through surface-diffusion and has an effect on the catalyst activity. The van der Waals force between particles and substrate are of comparable energy and are attributed to physical adsorption. These metal-substrate interaction energies may give less opportunity for CH_4 to attach to the metal surface for chemisorption.

Figure 2 (B) shows the Pd/Al_2O_3 sample reduced at 673K. The average particle size is estimated to be between 14-18 nm and form some cluster particles (crystallite) presumably arising from the coalescence mechanism. Twinning particles at the surface support are also formed. Most particles exist as crystallites on the support surface. These crystallites have active movement because the interaction between particles are higher compared to particle-support interaction energies. This situation may result in chemisorption of CH_4 on a more active metal surface, and higher conversion compared to 533K. The rate-limiting process for sintering here can be that of particle migration, or the process of coalescence, involving the growth of a neck between two particles and the gradual change in shape of the merged pairs into the lowest-energy configuration. The rates are determined by a number of factors. Basically these are related to the values of the metal-metal bond energies (and that of surface, edge, and corner atoms in contrast to those in the bulk metal) relative to the bond strength between metal and support.

Dissociation of particles from a crystallite occurs more readily if the particle-surface bonding is appreciable, but if this is too great, surface diffusion will be slow. Some portion of the detached particles must be mobile for surface diffusion-coalescence to occur. It appears that individual particles are weakly bonded to ionic surfaces and are therefore highly mobile.

Figure 2 (C) shows the sample treated under H_2-reduction for 3 hrs at 773K. It is obvious that the sample has undergone drastic changes in particle sizes, with a predominance of coagulated particles. The average particle size is estimated to be between 18-20 nm for individual particles. At this highest

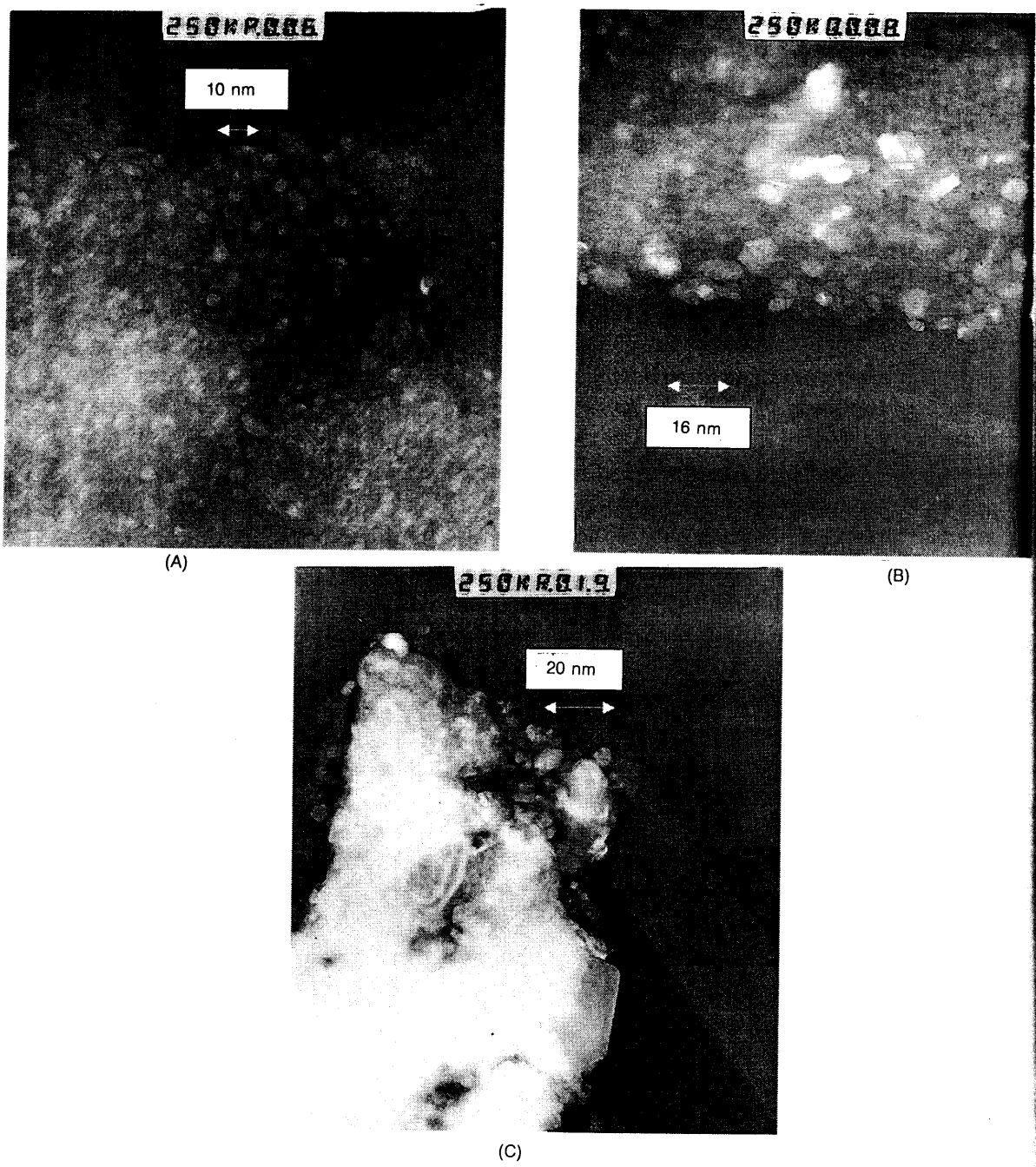

Figure 2 Microstructure Study Performed Using TEM at 250K Magnifications for Hydrogen Reduced 2 wt% Pd/Al_2O_3, at Different Reduction Temperatures (A) 533K, (B) 673K, and (C) 773K.

temperature studied, the interaction energy between particles becomes highest, thus the collision mechanism of particles occurs more readily and hence the

particle growth can be observed. These coagulated crystallites have diminished the metal dispersion and hence affected the CH_4 chemisorption. Twinning of particles is evident for some points on the support. This may result from a collision of particles, and the interaction energy obtained overcomes the energy of the movement of individual particles.

3.4 Catalyst Activity in the Chemical Kinetic Regime

For alumina-supported Pd catalyst, it has been determined that the kinetic rate is independent of oxygen [18, 19]. For methane concentrations in the range 0.1 to 6% volume, first order has been established [20, 21, 22, 23, 24]. Thus, the mass-specific reaction rate constant (k_m) can be calculated as follows [21, 25]:

$$k_m = -(F/m)[\ln(1 - x)] \tag{1}$$

where F/m is volumetric feed rate of the reactant divided by the weight of catalyst, i.e. the reciprocal of the space time, and x is the methane conversion.

It was assumed that the kinetic regime was achieved up to a maximum of 50% methane conversion for all supported catalysts. Arrhenius plots showed that linear relationships were obtained under 50% methane conversion [20], but there was a probability of diffusion controlled regime beyond 50% methane conversion, because of temperature gradients. Arrhenius plots were used to calculate the activation energy and pre-exponential factor for each sample condition. It is important that for catalyst performance comparison, each Arrhenius plot was developed below 50% methane conversion in order to achieve the kinetic regime, and to avoid the diffusion regime. The mass-specific reaction rate was calculated at 623K to allow direct comparison of the catalysts activities. The kinetic parameters of the activation energy, and pre-exponential factor were computed by the equation of;

$$k = Ae^{-E/(RT)} \tag{2}$$

where k is the specific reaction rate, cm^3g s, with temperature dependence, E is the activation energy, kJ per mol, A is the pre-exponential factor, or frequency factor, cm^3/g s, R is a gas constant, 8.314 kJ/mol K, and T is absolute temperature, K. By taking the natural logarithm of the equation (2),

$$\ln k = \ln A - E/R(1/T) \tag{3}$$

and an Arrhenius plot of $\ln k$ versus $(1/T)$ should be a straight line whose slope is proportional to the activation energy, and A is computed at the y-axis when $(1/T)$ is located to the origin point. The calculated activation energy was computed by using the decade method [26].

Calcined and reduced 2 wt% Pd/Al_2O_3 samples were tested for their catalytic performance under steady state condition from 0 to 100% methane conversion. The isothermal methane conversion were measured as a function of catalyst temperature as shown in Figure 3. The catalytic methane conversion started at different temperature for each catalyst, but all samples showed 100% conversion at high temperatures.

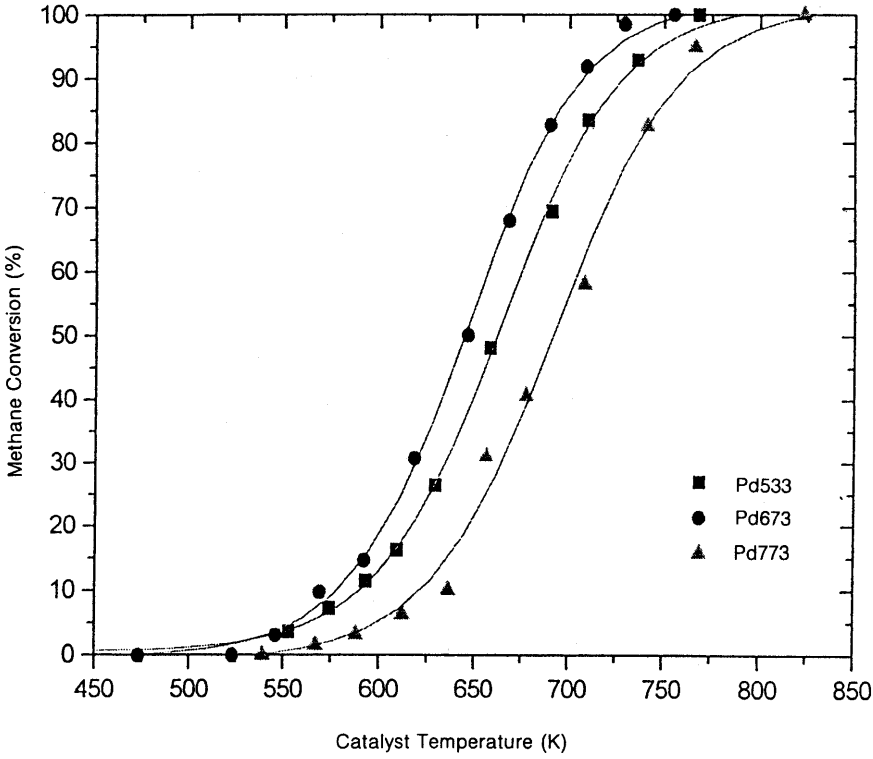

Figure 3 Methane Conversion (%) for 2 wt% H_2-reduced Pd/Al_2O_3 Catalysts

From the Arrhenius plots (Figure 4), the activation energies and pre-exponential factors for the apparent rate constants can be evaluated. For comparative purposes, the apparent mass-specific rate constants at 623K were also evaluated. The rate coefficients, $k_{m\ 623}$, together with the kinetic parameters of the activation energies, E_a and pre-exponential factors, A_o are shown in Table 4 for calcined and reduced samples. Calcined Pd/Al_2O_3 (CaPd) displayed the highest value of $k_{m\ 623}$, followed by Pd673, then Pd533, and lastly Pd773.

Both metallic, and ionic phases were present in all samples as shown in the XPS study. These phases may have different influences on the activation of

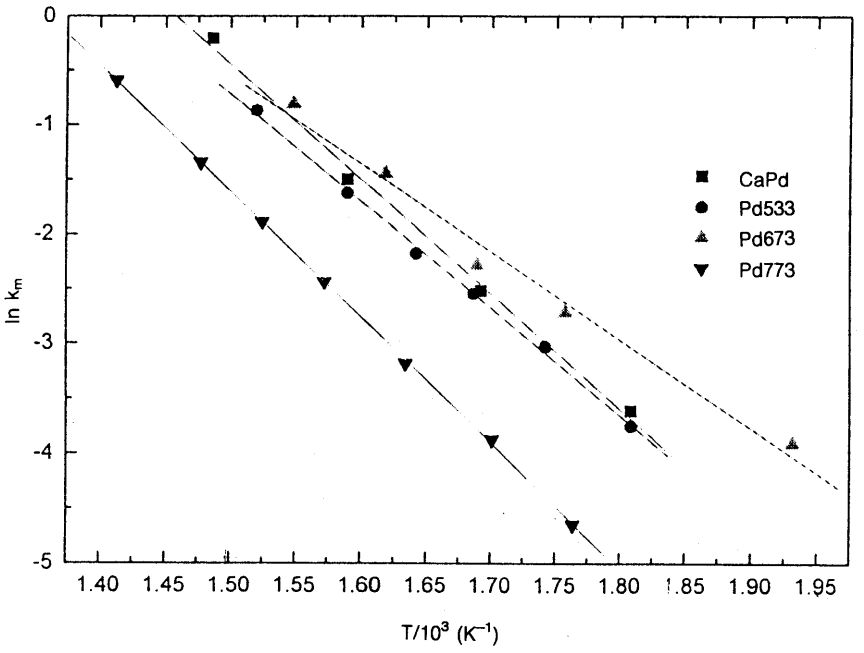

Figure 4 Arrhenius Plots for 2 wt% Calcined and H_2-reduced Pd/Al_2O_3 Catalysts

methane in the oxidation reaction. The metallic-ionic ratios in the calcined samples are used as the reference conditions as compared to the effect of different reduction temperatures.

For the reduced samples, the reduction temperatures changed their activity markedly. The pre-treatment step of the reduction modifies the nature of the catalyst and hence influences the catalyst performance. The catalysts modifications were demonstrated in the BET surface area, XPS, and TEM results. Table 4 shows the kinetic parameters produced for each catalyst, and the evaluated rate at 623K which is included for comparison. The catalytic activities of all the reduced catalysts were below of the calcined catalyst. However, among the reduced catalysts, reduction at 673K showed the highest catalyst activity compared to 533K and 773K. Reduced samples at 773K showed the worst activity which means that the nature of the catalyst has changed for the worst as a result of sintering (TEM). These observed catalyst activities can be correlated with the BET surface area, XPS and TEM studies which give information on the morphology and oxidation states of the reduced samples.

Table 4 Kinetic Parameters of Calcined and Reduced Samples Over 2 wt% Pd/Al_2O_3 for Methane Combustion

Samples	k_{623}/ $cm^3g^{-1}s_{-1}$	E_a/kJ mol^{-1}	$A_o/cm^3g^{-1}s^{-1}$	k_{623} Ratio (Reduced/Calcined)
CaPd	0.25	87	4.4×10^6	1.00
Pd533	0.17	82	1.2×10^6	0.68
Pd673	0.21	67	1.0×10^5	0.84
Pd773	0.06	96	6.2×10^6	0.24

Complete reduction of the ionic phases (probably PdO and Pd_2O) to Pd^o may happen for the all the reduction temperatures. The XPS results indicate that some metal re-oxidises under the atmosphere during the transfer of the samples from the plug flow reactor to the XPS equipment.

The pre-sintered metallic phase is responsible for methane oxidation on the heterogeneous surface. Quantitatively, the reduced palladium samples still have the highest catalyst activity compared to the other two reduced supported metals, especially for reduction at 673K. During the catalytic activity measurements this metallic phase could change back to PdO as previously noted [27] who suggested that in excess oxygen, oxygen is more strongly bonded to PdOx than hydrocarbon. The re-oxidation of PdO may occur at low temperature during the methane combustion. This PdO is more able than Pdo to chemisorb oxygen [28] which can be correlated to the higher condensation and sticking coefficient factors of the former. It has been suggested [29] that the PdO may exist in two different chemical states. One is an easily reducible PdO which is covered by metal particles, and the second is a stable oxide which interacts with alumina which may form isolated palladium aluminate [30]. Among the two chemical states, the first one is much more active than the oxide dispersed on the support [29, 30]. However the temperature for PdO dissociation could depend on the partial pressure of oxygen in the methane oxidation system [31].

As the reaction temperature increases, this PdO may be probably reduced again as follows,

$$2PdO_{(s)} \Longrightarrow 2Pd^{o}_{(s)} + O_{2(g)}$$

The chemical equation represents the free PdO dissociates at high temperature to form a metallic phase and oxygen, and this metallic phase can probably contribute to the adsorption of reactants to produce an activated complex.

During methane adsorption and reaction on the active surface, a redox mechanism has been proposed [32]. Firstly, there is strong oxygen adsorption on metallic particles leading to a surface palladium oxide. Secondly, there is adsorption and reaction of methane on this oxidic surface with the restoration of reduced palladium sites. Therefore, the palladium surface continuously changes from an oxidised state to a reduced state.

Calcined Pd/Al_2O_3 showed the highest activity compared to all reduced samples. It can be noted that the PdO plays an important role for the methane conversion. The decrease of catalyst activity at 533K and 773K is because the PdO has been completely reduced to the metallic phase. The increase of activity at 673K is probably the result of re-oxidisation of the metallic phase to PdO.

These different phases undoubtedly have different energy barrier for the adsorption of reactant species. The differences in the energy barrier of the different surfaces can be further correlated to the different condensation and sticking coefficient factors i.e. the hydrogen reduction temperatures have changed the energy barrier and hence changed the activation energies. For reduction at 773K, the crystallite growth increases and there is high resistance to adsorption, hence a high activation energy is required for the adsorption process. It is noted that the isolated metallic phase also contributes to a higher activation energy and pre-exponential factor compared to the dispersed phase. In this case, adsorption would be stronger, so that the formation of the surface complex would be more difficult.

4.0 SUMMARY

This study has shown that the different hydrogen reduction temperatures caused the change in surface area, oxidation state, and microstructure of the 2 wt% Pd/Al_2O_3. Calcined Pd/Al_2 showed the highest catalyst activity compared to hydrogen reduced samples. These reduced samples showed different activities in the combustion of methane which can be associated with different kinetic parameters. Reduction temperature at 673K showed the highest catalyst activity compared to 533K and 773K. Metallic and ionic species, and sintering phenomenon are the main factors in this study caused the change in catalyst activities.

5.0 ACKNOWLEDGEMENT

The authors would like to thank The Fuel and Energy Department, and Material Department, University of Leeds, for providing of research facilities of plug flow reactor, measurement of BET, XPS, and TEM with the guidance of Dr. J. M. Jones and Dr. R. Brydson.

REFERENCES

[1] Joo, H.L., D.L. Trimm and N.W. CantW. 1999. The Catalytic Combustion of Methane and Hydrogen Sulphide. *Catalysis Today*. 47: 353-357.

[2] Hicks, R.F., H. Qi, M.L. Young and R.G. Lee. 1990. Effect of Catalyst Structure on Methane Oxidation over Palladium on Alumina. *Journal Catalysis*. 122: 295.

[3] Yazawa, Y., H. Yoshida, N. Takagi, S. Komai, A. Satsuma and T. Hattori. 1998. *Applied Catalysis B; Environmental*. 19: 261.

[4] Maillet, T., C. Solleay, J. Barbier and D. Duprez. 1997. Applied Catalysis B; Environmental. 14: 85.

[5] Baldwin, T.R. R., and Burch. 1990. Catalytic Combustion of Methane over Supported Palladium Catalysts. *Applied Catalysis*. 66: 359.

[6] Cullis, C.F., and B.M. Willatt. 1983. Oxidation of Methane over Supported Precious Metal Catalysts. *Journal Catalysis*. 83: 267.

[7] Arai, H., and M. Machida. 1991. *Catalysis Today*. 10: 81.

[8] Bartolomew, C.H., and J.D. Butt. 1991. *Catalyst Deactivation*. 29.

[9] Mac Carty, J.G. 1994. *Scripta Metallic Material*. 31: 1115.

[10] Farrauto, R.J., M.C. Hobson, T. Kenelly and E.M. Waterman. 1992. *Applied Catalysis A*. 81: 227.

[11] Chen, J.J., and E. Ruckenstein. 1981. Sintering of Palladium on Alumina Model Catalysts in a Hydrogen Atmosphere. *Journal Catalysis*. 69: 254.

[12] Cullis, C.F., T.G. Nevell and D.L. Trimm. 1972. Role of the Catalyst Support in the Oxidation of Methane over Palladium. *Journal Chemical Society*. Faraday Transaction I. 68: 1406 and reference therein.

[13] Richardson, J.T. 1989. *Fundamental and Applied Catalysis: Principles of Catalyst Development*. New York and London: Plenum Press. 115.

[14] Moulder, J.F., W.F. Stickle, P.E. Sobol, P.E., and K.D. Bomben. 1995. *Handbook of X-Ray Photoelectron Spectroscopy: A Reference Book of Standard Spectra for Identification and Interpretation of XPS Data*.

[15] Somorjai, G.A. 1968. *X-Ray and Electron Methods of Analysis*. New York: Plenum. Chapter 6.

[16] Wanke, S.E., J.A. Szymura and T.T. Yu. 1987. The Sintering of Supported Metal Catalysts. *Catalyst Deactivation*. 65-95.

[17] Dalla Betta, R.A., and M. Boudart. 1972. *Proceeding 5th International Congress on Catalysis*. Miami Beach. North-Holland, Amsterdam. 1329.

[18] Veldsink, J.W., G.F. Versteeg and W.P.M. Van Swaaij. 1995. *Chem. Eng. Journal*. 57: 273-283.

[19] Baldwin, T.R., and R. Burch. 1990. Catalytic combustion of methane over supported palladium catalysts. *Applied Catalysis*. 66: 337-358.

[20] Hoyos, L.J., H. Praliaud and M. Primet. 1993. Catalytic combustion of methane over palladium supported on alumina and silica in presence of hydrogen sulphide. *Applied Catalysis A: General*. 98: 125-138.

[21] Yu, T.C., and H. Shaw. 1998. The effect of sulphur poisoning on methane oxidation over palladium supported on γ-alumina catalysts. *Applied Catalysis B: Environmental*. 18: 105-114.

[22] Briot, P., and M. Primet. 1991. Catalytic oxidation of methane over palladium supported on alumina. *Applied Catalysis*. 68: 301-314.

[23] Burch, R., F.J. Urbano and P.K. Loader. 1995. Methane combustion over palladium catalysts: the effect of carbon dioxide and water on activity. *Applied Catalysis A: General*. 123: 173-184.

[24] Burch, R., P.K. Loader and F.J. Urbano. 1996. Some aspects of hydrocarbon activation on platinum group metal combustion catalysts. *Catalysis Today*. 27: 243-248.

[25] Fogler, H.S. 1986. *Fundamentals of Chemical Reaction Engineering*. Prentice-Hall. Pg. 269.

[26] Fogler, H.S. 1992. *Elements of Chemical Reaction Engineering*. 2nd Edition. Prentice-Hall International Inc. Pg. 64.

[27] Yao, Y.F.Y. 1980. Oxidation of Alkines Over Noble Metal Catalysts. *Ind. Eng. Chem. Prod. Res. Dev.* 19: 293-298.

[28] Farrauto, R.J., M.C. Hobson, T. Kennedy and E.M. Waterman. 1992. *Applied Catalysis A.* 81: 227.
[29] Hicks, R.F., H. Qi, M.L. Young and R.G. Lee. 1990. *Journal of Catalysis.* 122: 280.
[30] Hoost, T.E., and K. Otto. 1992. *Applied Catalysis A.* 92: 39.
[31] Sekizawa, K., M. Machida, K. Eguchi and H. Arai. 1993. *Journal of Catalysis.* 142: 655.
[32] Garbowski, E., C. Feumi-Jantou, N. Mouaddib and M. Primet. 1994. *Applied Catalysis A.* 109: 277.